

Connexin-specific distribution within gap junctions revealed in living cells

Matthias M. Falk


Department of Cell Biology, The Scripps Research Institute, 10550 North Torrey Pines Road, La Jolla, CA 92037, USA
(e-mail: mfalk@scripps.edu)

Accepted 11 September; published on WWW 31 October 2000

SUMMARY

To study the organization of gap junctions in living cells, the connexin isotypes α_1 (Cx43), β_1 (Cx32) and β_2 (Cx26) were tagged with the autofluorescent tracer green fluorescent protein (GFP) and its cyan (CFP) and yellow (YFP) color variants. The cellular fate of the tagged connexins was followed by high-resolution fluorescence deconvolution microscopy and time-lapse imaging. Comprehensive analyses demonstrated that the tagged channels were functional as monitored by dye transfer, even under conditions where the channels were assembled solely from tagged connexins. High-resolution images revealed a detailed structural organization, and volume reconstructions provided a three-dimensional view of entire gap junction plaques. Specifically, deconvolved dual-color images of gap junction plaques assembled from CFP- and YFP-tagged connexins revealed that

different connexin isotypes gathered within the same plaques. Connexins either codistributed homogeneously throughout the plaque, or each connexin isotype segregated into well-separated domains. The studies demonstrate that the mode of channel distribution strictly depends on the connexin isotypes. Based on previous studies on the synthesis and assembly of connexins I suggest that channel distribution is regulated by intrinsic connexin isotype specific signals.

 Movies available on-line:
<http://www.biologists.com/JCS/movies/jcs1735.html>

Key words: Autofluorescent reporter technology, Cell-cell junction, Deconvolution (DV) microscopy, Green fluorescent protein (GFP), Oligomeric membrane protein

INTRODUCTION

A number of oligomeric proteins, including acetylcholine receptors, aquaporins, tight junction occludin and claudins, and gap junction channels, arrange into densely packed clusters, arrays or strands in the plasma membrane (McNutt and Weinstein, 1970; Friend and Gilula, 1972; Rash et al., 1974; Axelrod et al., 1976; Dunia et al., 1987; Peng, 1983; Yang et al., 1996; Tsukita and Furuse, 1999; Tsukita and Furuse, 2000). However, the signals that regulate their packing are poorly understood. Ultrastructural analyses revealed that gap junction channels, in particular, arrange extensively into two-dimensional sheets, or so-called gap junction plaques (McNutt and Weinstein, 1970; Friend and Gilula, 1972; Rash et al., 1974; Ginzberg and Gilula, 1979). Less than a dozen to many thousand individual channels can be combined into a single plaque that can extend from several nanometers to several micrometers in diameter (McNutt and Weinstein, 1970).

Gap junction channels represent double membrane protein structures that form by the head-to-head docking of two half-channels, termed connexons, to create hydrophilic pores across the membranes (Makowski et al., 1977). The channels mediate direct cell-to-cell communication by allowing the passage of small biological molecules (up to approximately 1 kDa) from one cell to the other (Gilula et al., 1972). Each connexon is composed of six polytopic transmembrane protein subunits, termed connexins (Cx). Therefore, only a single type of protein

is required, and is sufficient, to construct gap junction channels. At least 14 different connexin isotypes have now been cloned and sequenced from mice. All represent structurally conserved non-glycosylated members of a multigene family that mainly differ in their C-terminal domain (see Bruzzone et al., 1996a; Bruzzone et al., 1996b; Goodenough et al., 1996; Kumar and Gilula, 1996, for recent reviews). Although the different connexin isotypes exhibit a distinct tissue distribution, many cell types express more than one connexin isotype. This may allow the assembly of hetero-oligomeric connexons constructed from different connexin isotypes, in addition to the assembly of homo-oligomeric connexons constructed from a single connexin isotype.

Previous studies have shown that the connexin subunits are cotranslationally integrated into the endoplasmic reticulum (ER) membrane in a process that is similar to that described for other transmembrane proteins (Falk et al., 1994). There, the connexins adapt their native transmembrane configuration, traversing the membrane bilayer four times with N- and C-termini located in the cytoplasm (Falk and Gilula, 1998). Further studies demonstrated that connexins can assemble into functional hexameric connexons in the ER membrane (Falk et al., 1997). Subcellular fractionation studies (Musil and Goodenough, 1991; Falk et al., 1994) and immunocolocalization analyses (Musil and Goodenough, 1991; Laird et al., 1995) suggest that connexins pass through the Golgi apparatus to reach the plasma membrane. Connexons

are believed to dock in the plasma membrane to form the complete double-membrane channel structures, and channels cluster into gap junction plaques (reviewed by Yeager et al., 1998; Falk, 2000a; Falk, 2000b).

Many questions related to the biosynthesis and turnover of gap junction channels remain, however. Specifically, how and in which oligomeric or clustered stage are the connexins transported from the Golgi to the plasma membrane; where are the connexons integrated into the membrane; how do connexons in apposing membranes align and dock to initiate channel formation; what is the organization of the channels and why do they cluster; how is biosynthesis and function regulated and which signaling molecules are involved; and finally, what mechanisms are involved in gap junction turnover?

To address these questions in living cells, we tagged the gap junction proteins α_1 (Cx43), β_1 (Cx32) and β_2 (Cx26) with the autofluorescent tracer green fluorescent protein (GFP), and its cyan (CFP) and yellow (YFP) color variants, and combined this reporter technology with high-resolution fluorescence deconvolution (DV) microscopy, dual-color live cell and time-lapse imaging and three-dimensional volume rendering. Here I present (1) an extensive analysis of the tagged connexins after expression in the HeLa model cell-line, (2) a detailed three-dimensional view of entire gap junctions as they appear in the plasma membranes of living cells, and (3) how channels assembled from different connexin isotypes distribute within gap junction plaques.

MATERIALS AND METHODS

Connexin-GFP cDNA constructs

cDNA sequences of the autofluorescent reporter proteins CFP, GFP and YFP were fused in-frame to the C-terminus of rat α_1 (Cx43), human β_1 (Cx32) and rat β_2 (Cx26) cDNAs. The authentic connexin stop codons were deleted by PCR mutagenesis using proofreading native *PFU* Polymerase (Stratagene, La Jolla, CA, USA). Amplified connexin cDNAs were cloned into the *EcoRI* and *BamHI* restricted vectors pEGFPN1, pECFPN1 and pEYFPN1 (Clontech, Palo Alto, CA, USA). The resulting connexin constructs contained the 5'-untranslated connexin sequence of variable length (187 untranslated nucleotides in the α_1 [Cx43] construct, 62 untranslated nucleotides in the β_1 [Cx32] construct, and 48 untranslated nucleotides in the β_2 [Cx26] construct), the complete connexin specific coding sequence, a seven-amino-acid linker (Ala-Asp-Pro-Pro-Val-Ala-Thr) and the CFP, GFP or YFP coding sequence, respectively. All constructs were verified by restriction digest and automated DNA sequencing.

Cell lines, cell culture and transfection conditions

Human epitheloid cervix carcinoma cells (HeLa, ATCC CCL 2; American Type Culture Collection, Rockville, MD, USA) were used throughout this study. Chinese hamster ovary cells (CHO-K1, ATCC CCL 61), African green monkey kidney cells (COS-7, ATCC CRL1650), baby hamster kidney cells (BHK-21, ATCC CCL 10), embryonic mouse fibroblasts (3T3-Swiss albino, ATCC CCL 92), adenovirus 5-transformed human embryonic kidney cell line 293 (ATCC CRL 1573), liver oval cells (T51B, a gift of S. Shen, Northwest Hospital, Seattle, USA), and Madin Darby canine kidney cells (MDCK, ATCC CCL 34) were used as controls. Cell lines were maintained in standard cell culture medium supplemented with 10% fetal calf serum, and 100 i.u. penicillin and 100 U streptomycin per ml. For transfections, cells were split the day prior to transfection to reach 60-70% confluency. Cells were transfected with Superfect® Transfection Reagent (Qiagen, Valencia, CA, USA) following the

manufacturer's instructions. Transfection efficiencies of 10-30% were generally obtained with HeLa cells.

Thin section electron microscopy

HeLa cells were transiently transfected with GFP-tagged α_1 (Cx43) and incubated overnight. Cells were fixed in 2.5% glutaraldehyde, 0.1 M sodium cacodylate buffer, pH 7.3, 1 mM CaCl₂, for 45 minutes at room temperature (RT) and, after washing 3 times with 0.1 M cacodylate buffer, with 1% osmium tetroxide in 0.1 M cacodylate buffer (for 1 hour at RT). After washing in 0.1 M cacodylate buffer (3 times) cells were treated in 0.5% tannic acid (30 minutes at RT), 1% Na₂SO₄ in 0.1 M cacodylate buffer (10 minutes at RT), followed by a rinse in 0.1 M cacodylate buffer. Cells were dehydrated in an ethanol series following an initial incubation in 1% uranyl acetate in 10% ethanol (15 minutes at RT) followed by a final treatment in 2-hydroxypropylmethacrylate (Electron Microscopy Sciences, Fort Washington, PA, USA). Cells were flat-embedded in LX-112 (Ladd Research Industries Inc., Burlington, VT, USA) and incubated overnight at 60°C. Embedded cells were mounted, thin-sectioned and examined with a Philips CM100 electron microscope.

Immunoblot analysis

Total cell homogenates of transfected cells were separated without boiling on 10% SDS-Mini protein gels (BioRad, Hercules, CA, USA), transferred onto nitrocellulose membranes, and blocked with 5% dry milk. Purified α_1 (Cx43) specific polyclonal antipeptide antibodies (α_1 S) (Milks et al., 1988), a monoclonal antipeptide antibody specific for the C-terminal amino acid residues of β_1 (Cx32) (β_1 SB8), and a monoclonal antipeptide antibody specific for a portion of the intracellular loop domain of β_2 (Cx26) (β_2 JD5) (Risek et al., 1994) were kindly provided by N. B. Gilula (The Scripps Research Institute, La Jolla, CA, USA). A polyclonal anti-GFP antibody was obtained from Clontech Laboratories. Primary antibodies were used at 1:1000 dilution, horseradish peroxidase-coupled secondary goat anti-rabbit (BioRad) and goat anti-mouse (Pierce, Rockford, IL, USA), respectively, were used at 1:15,000 dilution. Bound antibodies were detected by enhanced chemiluminescence (Pierce).

Immunofluorescence staining

HeLa cells were seeded on microscope coverglasses treated overnight with poly-L-lysine solution (Sigma, St Louis, MO, USA), transfected, and incubated overnight. Cells were fixed for 10 minutes at RT in 2% formaldehyde (Polysciences Inc. Warrington, PA, USA), permeabilized in ice-cold acetone (5 minutes at -20°C), blocked (30 minutes at RT in 1× PBS containing 1% bovine serum albumin), washed 3 times in 1× PBS, and incubated with primary antibodies (described above) diluted 1: 100 in 1× PBS containing 0.5% BSA (1 hour at RT). Monoclonal anti-Golgi p58K protein (Sigma) and polyclonal anti-calnexin antibodies (StressGen, Victoria, BC, Canada) were used at 1:100 dilution. Cy3-coupled goat anti-rabbit and goat anti-mouse (Jackson Laboratories, West Grove, PA, USA), respectively, were used as secondary antibodies at 1:200 dilution. Nuclei were stained with DAPI before mounting in Fluoromount-G (Southern Biotechnology Associates Inc., Birmingham, AL, USA). Cells were examined with a Zeiss Axiophot fluorescence microscope equipped with a 100× (Plan-Neofluar NA 1.3 oil immersion) objective lens and standard filter sets. Single, double and triple exposures were imaged on Kodak 1600 ASA slide film.

Dye transfer analysis

To examine dye transfer capabilities of tagged gap junctions in HeLa cells, medium was exchanged with pre-warmed 1× PBS and dishes were placed on a stage heated to 37°C mounted on an inverted epifluorescence microscope (Zeiss Axiovert 100). Clusters and pairs of cells expressing GFP-labeled gap junction plaques were selected, single cells of the clusters with gap junction plaques visible by fluorescence illumination in their plasma membranes were

microinjected with 5% solutions of either Lucifer Yellow, Cascade Blue or Sulforhodamine (Molecular Probes, Eugene, OR, USA) and imaged with a 60 \times long-distance objective lens (Olympus LC Plan FL, NA 0.70). Representative injection experiments ($n > 20$ per connexin isotype) are shown. Non-transfected HeLa cells in the same dishes were injected as controls ($n > 20$).

Deconvolution microscopy and image processing

To obtain high-resolution images and three-dimensional volume reconstructions of gap junctions in live cells a deconvolution microscope system (DeltaVision Model 283, Applied Precision Inc., Issaquah, WA, USA) was implemented. DeltaVision's deconvolution process computationally reassigns the fluorescent blur generated by out-of-focus fluorescence and lens aberration to its source using an inverse matrix algorithm, namely the constrained iteration method developed by Agard and Sedat (Agard et al., 1989) to noticeably enhance the resolution of the images (see Shaw, 1998; Falk and Lauf, 2000, for methodology reviews). HeLa cells were seeded on poly-L-lysine-treated coverglasses (Biotech Inc. Butler, PA, USA) and transfected with tagged connexins. The next day, coverglasses were mounted in a closed live-cell chamber (Focht Live-Cell Chamber System FCS2, Biotech Inc.) using Phenol Red-free DMEM (Gibco BRL, Grand Island, NY, USA). Temperature was kept constant at 37°C using the attached automatic FCS2 temperature controller. A Kodak Photometrics, CH350L liquid-cooled charged-coupled device (CCD) camera (500 KHz, 12 bit, 1317 \times 1035 pixels) was used for imaging, attached to an inverted, wide-field fluorescence microscope (Olympus IX-70). The autofluorescent tracer proteins CFP, GFP and YFP were excited with a standard mercury arc lamp attached to a fiber optic illumination scrambler providing even illumination. GFP fluorescence was detected using a standard FITC filter set. CFP and YFP fluorescence was imaged alternating using an 86002 filter set (Chroma Technology Corp., Brattleboro, VT, USA). Optical sections of gap junction plaques were acquired at maximum magnification (1500 \times , PlanApo 100 \times , NA 1.35 oil immersion lens, plus 1.5 \times auxiliary magnification). Section planes were collected in 0.2 μ m steps covering the entire gap junction in a z-axis field of 5–10 μ m using the attached Applied Precision Inc. high-precision motorized stage. Images were acquired, setting binning and gain of the CCD camera to 1, resulting in a minimum pixel size corresponding to 44.8 \times 44.8 nm (approx. 5 \times 5 gap junction channels) of the specimen. In some experiments the relatively low signal and bleaching-tendency of CFP required setting the gain to 4 to obtain adequate exposure times. In general, 0.2–0.5 second exposure times were sufficient to obtain images suitable for deconvolution with GFP ($\geq 1,100$ gray levels; dynamic range of the cooled CCD camera was 0–4095). Exposure times were between 0.2–1 seconds for YFP and 2–6 seconds for CFP. Images were saved and processed on attached Silicon Graphics workstations (O2, Octane) using the DeltaVision software package *softWoRx* (Version 2.5), and stored on CD-ROM.

Online supplemental material

Five QuickTime movie sequences featuring animated three-dimensional volume renderings of entire gap junction plaques imaged in living cells are included with this paper.

RESULTS

GFP-tagged connexins traffic and assemble efficiently into gap junction channels and typical gap junction plaques

To study the organization of gap junctions in live cells, the C-termini of three major connexin isoforms α_1 (Cx43), β_1 (Cx32) and β_2 (Cx26) were tagged with the autofluorescent reporter GFP. GFP-tagged connexins assembled into typical gap

junction plaques that were visible by fluorescence microscopy as green fluorescent puncta and lines in the adjoining plasma membranes of transfected HeLa cells (marked with arrows in Fig. 1A). GFP expressed alone was not targeted and filled the entire cell (Fig. 1A, bottom right panel). The size of the plaques correlated with the connexin isotype, and time of expression. Identical plaques were also assembled in other communication-competent and -deficient cell lines, such as CHO, COS-7, BHK, NIH 3T3, 293, T51B and MDCK cells, which were either transiently or stably transfected. HeLa cells were chosen for all further studies presented here since they have been shown to efficiently assemble functional gap junctions when transfected with connexin-specific cDNAs (Elfgang et al., 1995), they do not express endogenous α_1 (Cx43), β_1 (Cx32) or β_2 (Cx26) (Eckert et al., 1993; Elfgang et al., 1995; Hülser et al., 1997), and their growth is not contact-inhibited. The latter results in the formation of gap junctions viewable onto their surface, besides the more common view onto the edge of the plaques.

Expression of GFP-tagged α_1 (Cx43) was observed first 4–5 hours post-transfection as diffuse fluorescence throughout the cell body (cells marked with asterisks in Fig. 1B, 4h) that then accumulated in an area next to the nucleus (marked with arrows in the images 4h and 5h in Fig. 1B). Protein localization studies indicated that α_1 (Cx43) localized to the ER and Golgi (see below). The first gap junctions were formed 4–6 hours post-transfection as a single (arrowhead in Fig. 1B, 5h) or a few small fluorescent spots (Fig. 1B, 5h and 6h). Time-lapse recordings (M. Falk, unpublished data) indicated that, over time, smaller plaques increased in size or fused by moving laterally within the plane of the membranes. After longer expression times plaques could grow very large, filling large areas of the adjoining membranes (Fig. 1B, 40h). 50–60 hours post-transfection, when transcription had diminished from transiently transfected plasmids, only small gap junction plaques were left (Fig. 1B, 60h), which were degraded after 80 hours post-transfection under these experimental conditions (Fig. 1B, 80h). Similar plaque assembly and degradation kinetics were obtained with GFP-tagged β_1 (Cx32) and β_2 (Cx26).

Gap junctions assembled from GFP-tagged connexins also appeared normal by high-resolution structural criteria. Typical gap junction plaques with continuously joined plasma membranes throughout the area of the junctional membrane, the central gap, the 7-stripped staining pattern, and no obvious connections to cytoskeletal elements were visible in thin section electron micrographs of HeLa cells transiently transfected with α_1 (Cx43) (Fig. 1C). Gap junctions assembled from GFP-tagged α_1 (Cx43) appeared similar in width to gap junctions assembled from wild-type connexin (17–20 nm). This is a result of the staining technique that only insufficiently contrasts the GFP polypeptides. No gap junctions were detected in untransfected HeLa cells.

Tagged connexins were further examined by immunoblot analysis using connexin, as well as GFP-specific antibodies. Protein bands with an electrophoretic mobility of approximately 70 kDa, 59 kDa, 53 kDa, and 27 kDa, corresponding to α_1 (Cx43)-GFP, β_1 (Cx32)-GFP, β_2 (Cx26)-GFP and GFP alone, respectively, were detected in transfected HeLa cells (Fig. 2A, lanes 1, 2, 4, 6, 8–11). No such protein bands were detected in mock transfected cells (Fig. 2A, lanes 3, 5, 7, 12). Also, no

protein bands corresponding to endogenous connexins or GFP alone were detected (Fig. 2A, lanes 1-10). Slower migrating protein bands were detected in longer exposures of α_1 (Cx43)-GFP transfected cells (marked with an arrow in Fig. 2A, lane 2). They correlate with the phosphorylated forms of wild-type

α_1 (Cx43) (Musil and Goodenough, 1991; Laird et al., 1991; Laird et al., 1995). Some faster migrating protein bands probably representing degradation products were detected with all three connexin isotypes in longer exposures as well (marked with asterisks in Fig. 2A, lane 2; shown for α_1 [Cx43]-GFP only).

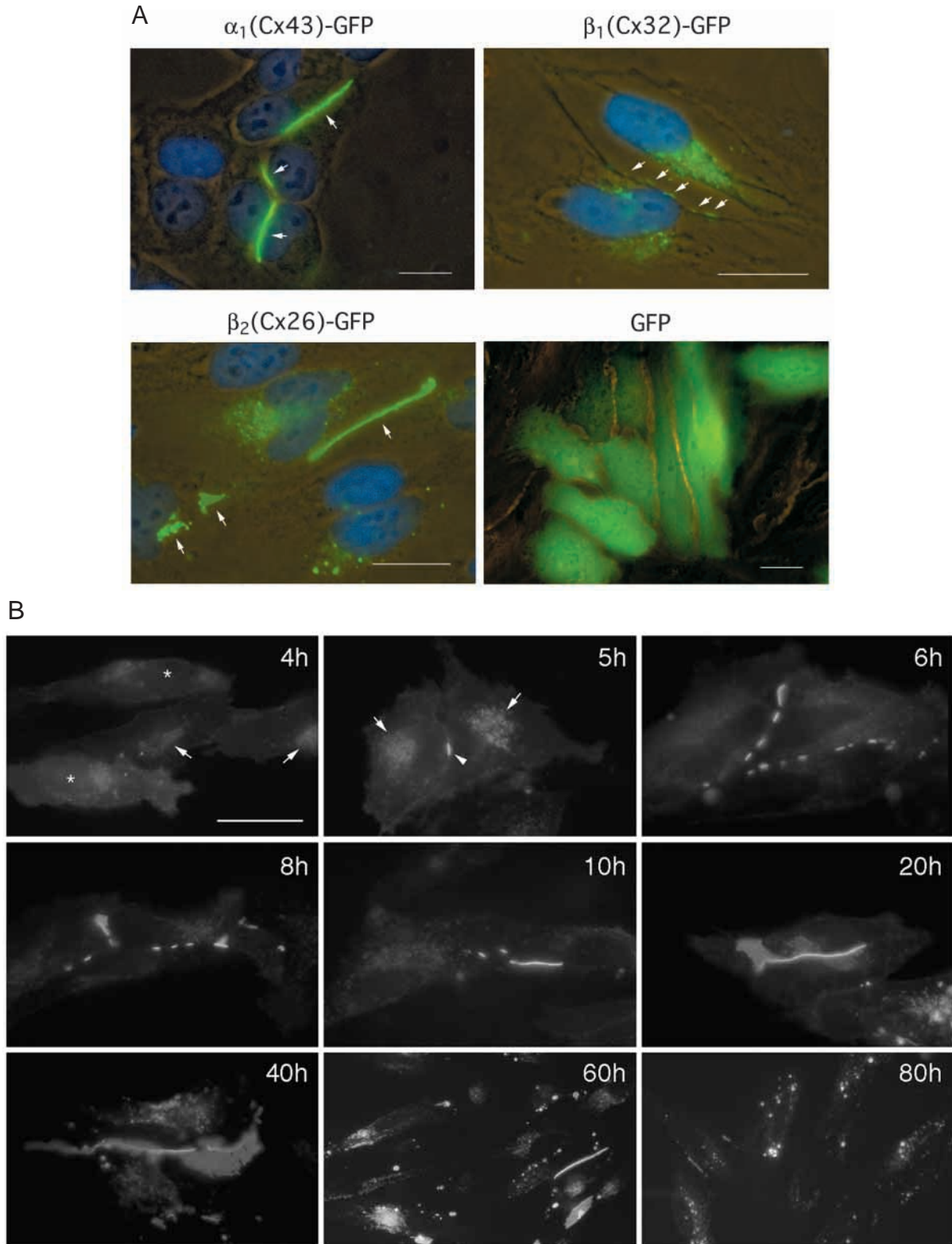


Fig. 1

C

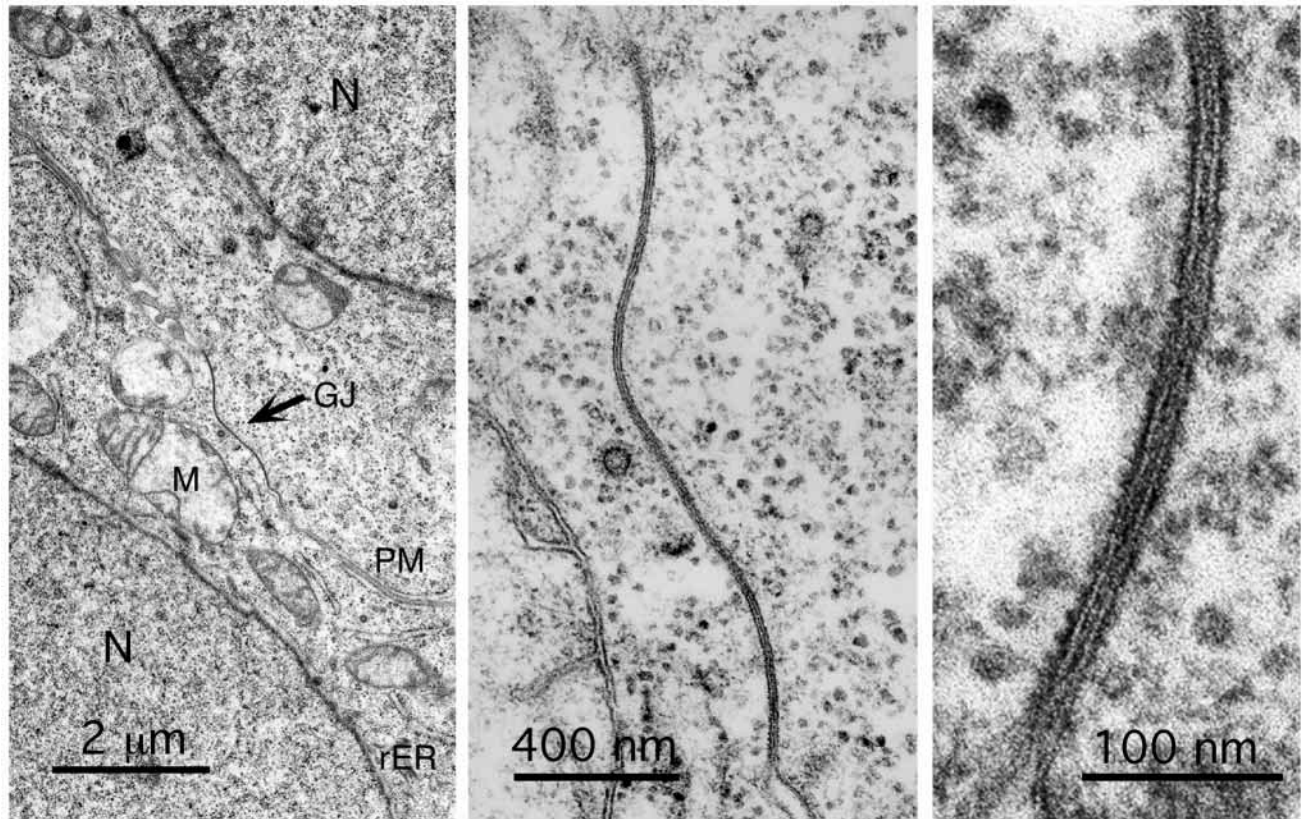


Fig. 1. GFP-tagged connexins assemble into typical gap junctions. (A) HeLa cells were transiently transfected with GFP-tagged connexins α_1 (Cx43), β_1 (Cx32) and β_2 (Cx26) and imaged 16–20 hours post-transfection. Gap junction plaques assembled in the adjoining plasma membranes of neighboring cells are visible as green lines and puncta (labeled with arrows). Note the different sizes and fluorescent intensities of the plaques. Nuclei are stained with DAPI (blue). Fluorescence was imaged successively with FITC and DAPI filter sets, followed by phase-contrast illumination. Cells transfected with GFP alone exhibited typical cytoplasmic fluorescence. (B) Kinetic analysis of gap junction assembly and degradation. HeLa cells transiently transfected with α_1 (Cx43)-GFP were observed for 80 hours. Representative cells from one dish were imaged at the time points post-transfection indicated on the images. Diffuse fluorescence throughout the cell body was detected first (4h, asterisks), which then accumulated next to the nucleus (arrows) before the first gap junctions (5h, arrowhead) were assembled. Bar, 20 μ m. (C) Ultrastructural analysis of thin-sectioned HeLa cells transfected with α_1 (Cx43)-GFP. Cells were fixed 16 hours post-transfection. Gap junction plaques of typical appearance were found (arrow in left panel) and shown at higher magnification in middle and right panels. No gap junction plaques were found in non-transfected HeLa cells. GJ, gap junction; M, mitochondria; N, nuclei; PM, plasma membrane; rER, rough endoplasmic reticulum.

In immunostained HeLa cells transfected with GFP-tagged α_1 (Cx43), β_1 (Cx32), and β_2 (Cx26), all detectable GFP fluorescence (Fig. 2B, column 1, green) corresponded to connexins fluorescently labeled with connexin-specific antibodies (Fig. 2B, column 2, red), resulting in a complete overlap of the two chromophores (Fig. 2B, column 3, yellow). Representative cells typically seen on the slides in repetitive experiments are shown.

Some intracellular localized connexin-GFP fluorescence was observed in the transfected cells as well (e.g. Figs 1A,B, 2B). To examine whether these connexins may represent transport intermediates in transit to the plasma membrane, double-labeling experiments of connexin-GFP and ER or Golgi membranes were performed. Antibodies directed against calnexin, an ER resident, and p58, a Golgi resident protein were used with secondary antibodies coupled to Cy3 (red) (Fig. 2C). A typical staining of ER and Golgi membranes in fixed HeLa cells is shown in the left panels. On the right, HeLa cells

transiently transfected with α_1 (Cx43)-GFP are shown. In transfected cells with green fluorescent gap junction plaques in their adjoining plasma membranes, intracellular located connexin-GFP (green) colocalized with ER and Golgi compartments (red), resulting in yellow, connexin-GFP-containing ER and Golgi membranes, respectively. Similar images were obtained for GFP-tagged β_1 (Cx32) and β_2 (Cx26), and with protein disulfide isomerase (ER-specific) or Mannosidase II (Golgi-specific) antisera.

Gap junction channels assembled from GFP-tagged connexins are functional

To investigate whether connexins tagged with GFP form functional gap junction channels, classical dye transfer experiments using gap junction permeable dyes were performed. Confluent monolayers of HeLa cells were transiently transfected with GFP-tagged α_1 (Cx43), β_1 (Cx32) or β_2 (Cx26) (shown in Fig. 3A,D,G,K). Individual cells in a

Fig. 2. Characterization of gap junctions assembled from GFP-tagged connexins. (A) Western blot analysis of HeLa cells transfected with GFP-tagged connexins. Connexin-GFP fusion proteins were detected in transfected cells with connexin (Cx), and GFP-specific antibodies (lanes 1, 2, 4, 6, 8-10). No connexins, GFP or fusion proteins were detected in untransfected (mock) cells. GFP was detected in the control transfection (lane 11). Phosphorylated forms of α_1 (Cx43) (arrow), and some degradation products (asterisks) were detected in longer exposures as well (lane 2). Protein size markers are shown on the right. (B) Colocalization of GFP fluorescence detected in Cx-GFP transfected HeLa cells (column 1) with connexin protein (column 2). Double exposures are shown in column 3. (C) Intracellular connexin-GFP colocalizes with rough endoplasmic reticulum (rER) and Golgi membranes. rER and Golgi membranes were visualized in HeLa cells with marker proteins as indicated (red). α_1 (Cx43)-GFP derived gap junction plaques are shown in green. Intracellular located α_1 (Cx43)-GFP colocalizing with rER or Golgi membranes appear yellow. Nuclei are stained with DAPI (blue). Successive triple exposures are shown on the right. Stained rER and Golgi membranes in fixed, non-transfected HeLa cells are shown in controls on the left. Bars, 20 μ m.

group, or a pair of transfected cells were microinjected. Cells were imaged before (Fig. 3B,E,H), and shortly after (1-3 minutes) dye injection (Fig. 3A,C,F,I,K). The dye spread within seconds to the neighboring cells only when gap junctions assembled from GFP-tagged connexins were present. Dye did not spread to adjacent untransfected cells of the monolayer even after prolonged incubation times (16 hours at 37°C). Untransfected HeLa cells not expressing connexins (marked with an asterisk in Fig. 3A) did not transfer dye either. Dye transfer was immediate (1-2 seconds) in α_1 (Cx43)-GFP and β_1 (Cx32)-GFP expressing cells, and somewhat delayed (2-5 seconds) in β_2 (Cx26)-GFP expressing cells. Similar results were also obtained with other gap junction permeable dyes, such as Cascade Blue or Sulforhodamine.

Taken together, these results demonstrate that connexins, tagged with GFP on their C-terminus, trafficked, assembled and clustered normally into functional gap junction channels and typical gap junction plaques.

Structural organization of gap junctions in living cells

To investigate the organization of gap junctions and to reconstruct three-dimensional views of entire gap junctions as they appear between living cells, GFP-tagged connexins were expressed in HeLa cells, and assembled gap junctions were imaged in living cells by high-resolution fluorescence deconvolution

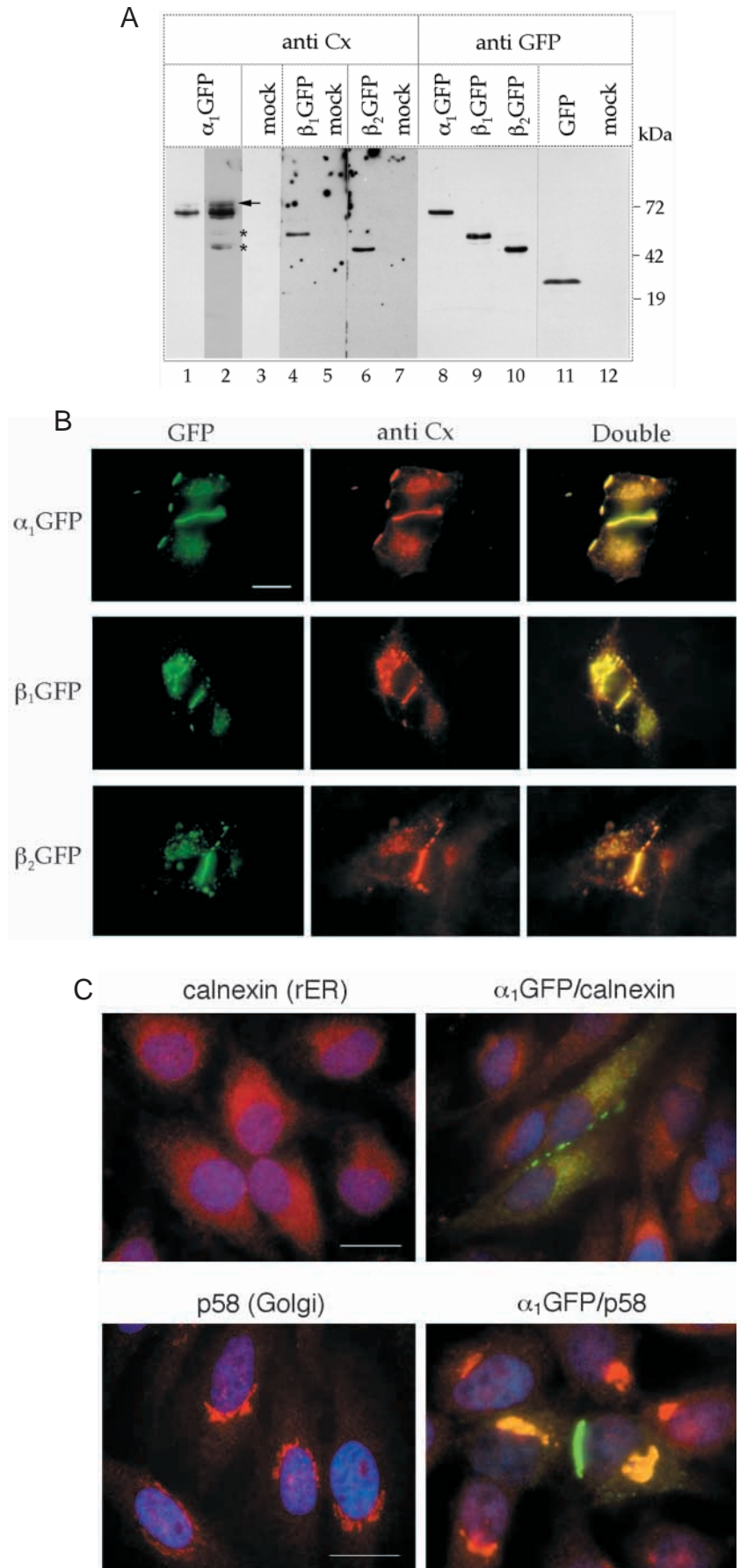
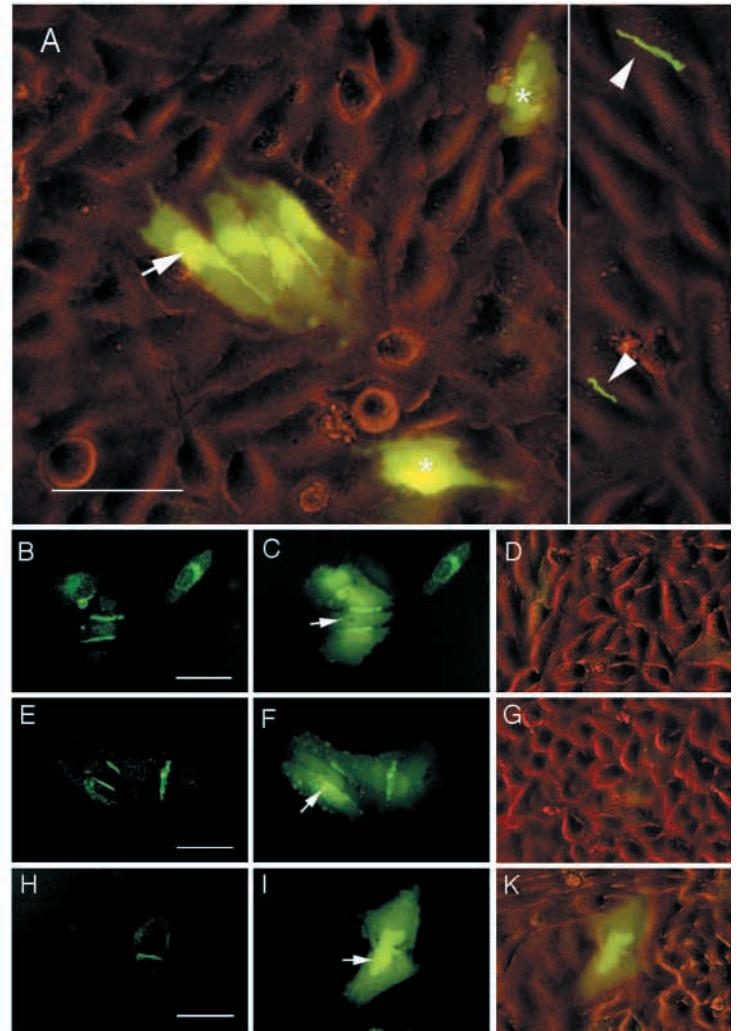


Fig. 3. GFP-tagged connexins form functional gap junction channels. A single cell in a cluster of transiently transfected HeLa cells (arrows in A,C,F,I) was microinjected with Lucifer Yellow. Non-transfected HeLa cells injected as control (asterisks in A) are unable to transfer dye. Gap junction plaques between non-injected cells are marked with arrowheads. Two areas of the monolayer, located close to each other are shown in A. In (B,E,H), cells were imaged before dye injection; in (A,C,F,I), after injection. Fluorescence emission and phase contrast were imaged simultaneously in A and K, while representative areas of the monolayers are shown in D and G. Bars, 50 μm .



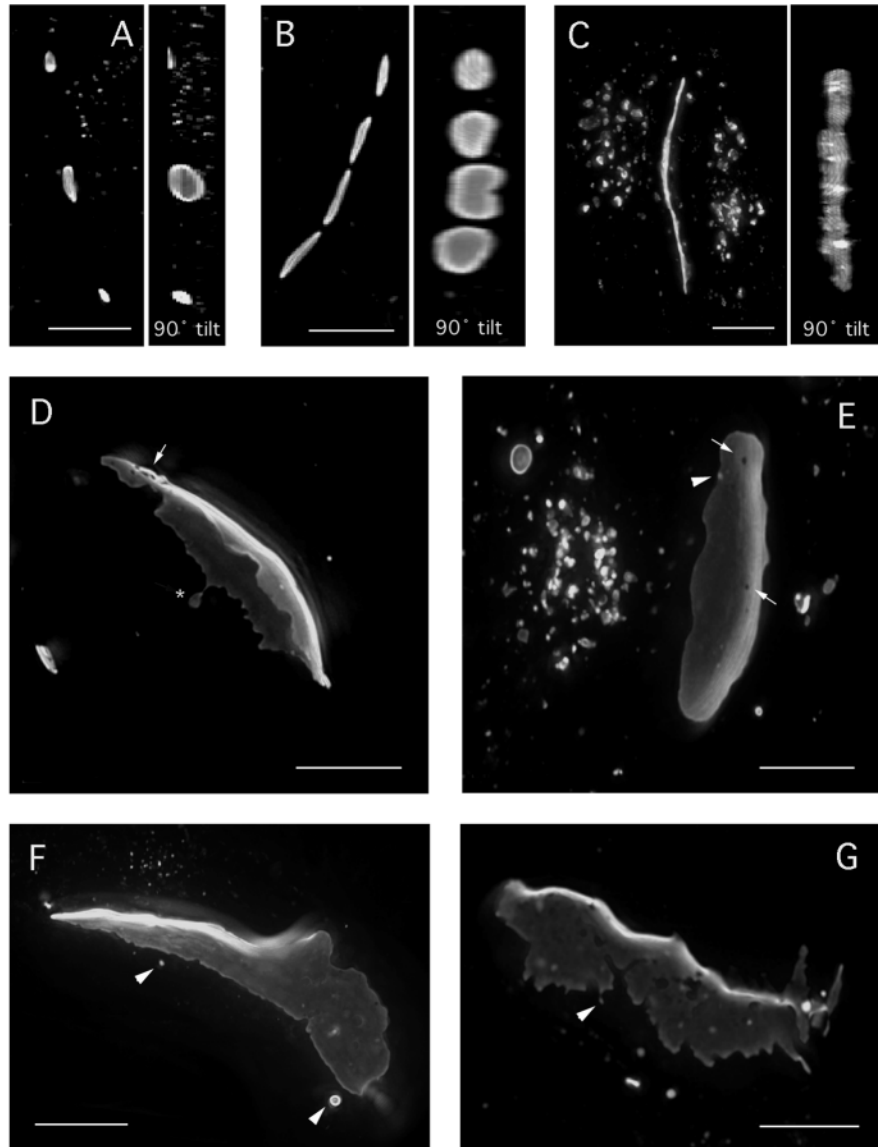
microscopy. Stacks of consecutive microscopic z -sections were acquired from gap junction plaques either visible onto their edge, or onto their surface, respectively, covering the entire depth of the plaques. Images were deconvolved, and three-dimensional volume reconstructions were rendered from the z -sections using *softWoRx* computer software that then were rotated around their longitudinal axis. A selection of such volume views of smaller ($\leq 2 \mu\text{m}$ diameter) and larger ($\geq 5 \mu\text{m}$ diameter) gap junction plaques assembled from GFP-tagged α_1 (Cx43) is shown in Fig. 4, and animated in the QuickTime movie sequences 1-5. Gap junction plaques were found to be quite diverse in appearance. In general, plaques were irregular in shape rather than circular. The edges of the plaques were usually wavy or jagged, and sometimes long protrusions (asterisk in Fig. 4D) or deep invaginations deprived of gap junction channels extended from their edges. Circular, as well as irregular-shaped areas (approx. $0.1\text{-}1 \mu\text{m}$ in diameter) lacking gap junction channels were detected within the gap junction channel plaques (arrows in Fig. 4D,E). Furthermore, fluorescent vesicles were detected in intracellular compartments such as rER and Golgi membranes (Fig. 4A,C,E), on the edges (arrowhead in Fig. 4E), and in close vicinity of the plaques (arrowheads in Fig. 4F,G). Note that some of the more complex gap junctions shown in Fig. 4D,F,G, and in the QuickTime movie sequences 3-5 appear more fluorescent in their center where the plaques are imaged onto their edges. This is due to the imaging technique and does not reflect a true increase in fluorescence. In the plane view areas of the plaques only two layers of GFP, located on either side of the channels, are present per section (see Discussion and Fig. 7). Approximately 20 channels including their GFP tags are present per section in the areas where the plaques were sectioned through their edges.

Structural composition of gap junctions assembled from more than one connexin isotype

To investigate whether different coexpressed connexin isotypes would gather within the same junctional plaque and how they would distribute, the connexin isotypes α_1 (Cx43), β_1 (Cx32) and β_2 (Cx26) were tagged with the GFP color variants CFP and YFP, respectively. Tagged connexins were coexpressed in

all possible combinations in transfected HeLa cells. Both connexin isotypes gathered within the same junctional membrane areas and assembled into gap junction plaques that contained both connexin isotypes. When tagged β_1 (Cx32) was cotransfected with tagged β_2 (Cx26), the two proteins were distributed homogeneously throughout the entire plaque, resulting in homogeneously yellow plaques (Fig. 5, row 2). When tagged α_1 (Cx43) and β_1 (Cx32), or α_1 (Cx43) and β_2 (Cx26) were coexpressed, still both proteins gathered within the same gap junction plaques, however, completely segregated into well-separated domains (green, or red) consisting of either connexin isotype (Fig. 5, rows 3,4). Identical results were obtained with exchanged tags. To further eliminate the possibility that the protein tags were responsible for this specific channel distribution, cells were cotransfected with two cDNAs encoding the same connexin isotype, but tagged either with CFP or YFP, respectively. In all these instances, the tagged connexin isotypes were distributed evenly, resulting in homogeneously yellow plaques (shown for α_1 [Cx43]-CFP/ α_1 [Cx43]-YFP in Fig. 5, row 1). Segregation was independent of plaque size – small (Fig. 6A) and larger plaques (Figs 5, 6B) showed identical segregation and ratio of the two expressed connexins, as shown for coexpressed α_1 (Cx43)-YFP/ β_2 (Cx26)-CFP in Fig. 6B.

Fig. 4. Three-dimensional volume reconstructions of gap junctions. Structural features of the plaques such as wavy and jagged edges, invaginations (as in G), protrusions (asterisk in D), regular and irregular shaped areas not containing gap junction channels (dark areas within bright areas, arrows in D and E) are clearly resolved. Fluorescent vesicles are present on the edge (arrowhead in E) in the close vicinity of the plaques (arrowheads in F,G) and in intracellular compartments, such as rER and Golgi membranes (A,C,E). That gap junction plaques represent two-dimensional sheets extending throughout the plane of the membrane is clearly demonstrated by this technique. (D-G) More complex gap junction plaques with 'U' or 'L'-shaped cross-section profiles. Plaques are shown in the projection angle in which images were acquired, and with a 90° tilt in A-C. Bars, 5 μ m. (See also attached QuickTime movie sequences for animated presentations.)



DISCUSSION

Three different connexin isotypes, α_1 (Cx43), β_1 (Cx32) and β_2 (Cx26), were tagged with the autofluorescent proteins CFP, GFP and YFP and this reporter technique was combined with single and dual-color, high-resolution fluorescence deconvolution (DV) live-cell microscopy and volume rendering. This approach permitted a study of the structural organization and the distribution of channels within gap junction plaques assembled from one or two different connexin isotypes in living cells.

Functional integrity of GFP-tagged gap junction channels

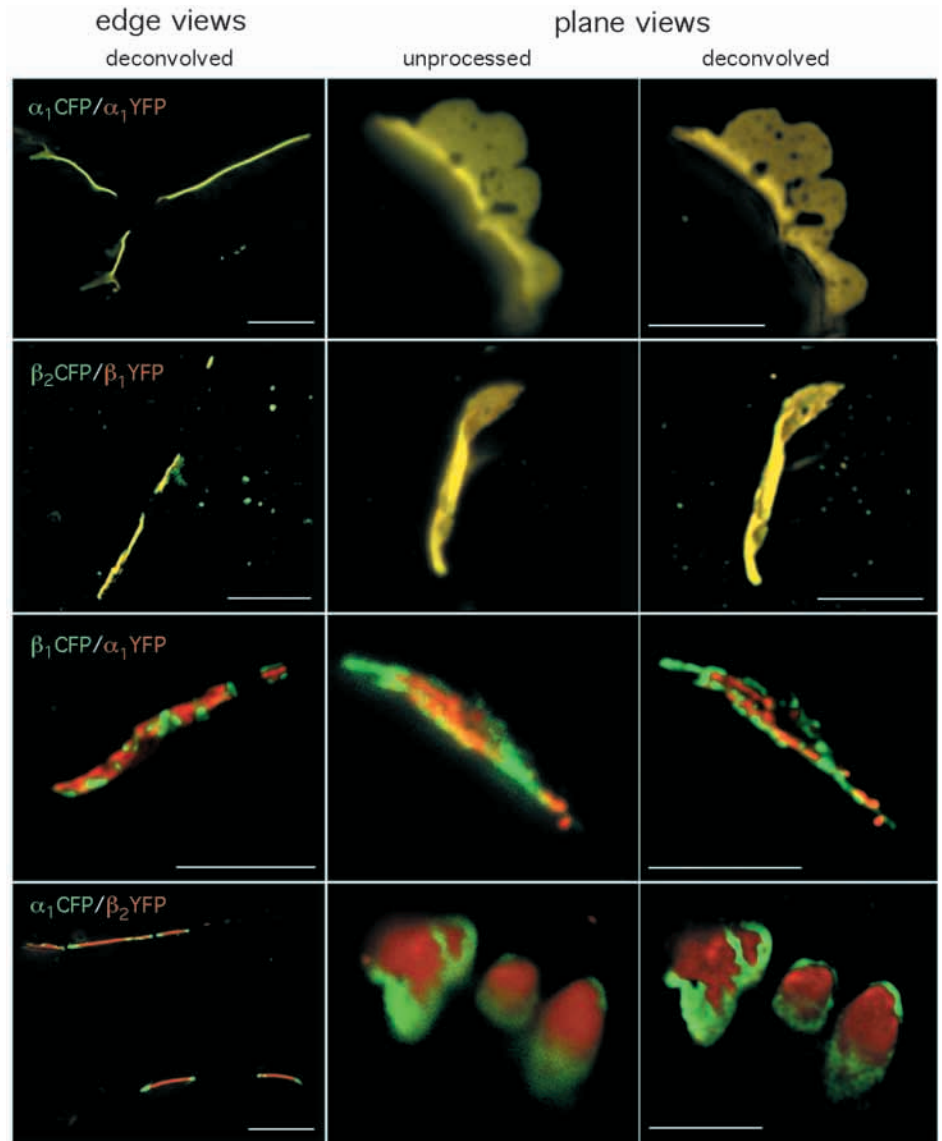
When the tagged connexins were expressed in transfected HeLa or other communication-competent or -deficient cell lines, they assembled into functional gap junctions that appeared indistinguishable by structural and ultrastructural analysis from wild-type gap junctions. Dye microinjection analysis indicated that the tagged channels allowed the passage of gap junction permeable dyes, as described for wild-type gap junction channels. Further, Bukauskas et al. (2000) found that the electrical properties of channels assembled from GFP-tagged α_1 (Cx43) were identical to those of wild type α_1 (Cx43), except for a reduced sensitivity to transjunctional voltage.

Further, it was found that the size of the gap junction plaques, in general, correlated with the connexin isotype. Gap junctions assembled from α_1 (Cx43)-GFP, in general, formed more solid, brightly fluorescent plaques, which over time could grow very large (≥ 10 μ m diameter). Gap junctions assembled from β_2 (Cx26)-GFP formed less fluorescent plaques, which grew to intermediate sizes (≤ 10 μ m diameter). Gap junctions assembled from β_1 (Cx32)-GFP generally remained small (≤ 2 μ m diameter), often only visible as a line of relatively faint

puncta. Whether the GFP tag may reduce efficiency of β_1 (Cx32) transport and/or assembly, and by this influences β_1 (Cx32) gap junction plaque size, was not further investigated. Interestingly, however, β_1 (Cx32) assembled into larger plaques (5-10 μ m in diameter) when it was coexpressed with another connexin isotype, such as α_1 (Cx43) or β_2 (Cx26) (see Fig. 5). Large gap junction plaques (≥ 10 μ m diameter) were found in different tissues, such as the otocyst sensory epithelium (Ginzberg and Gilula, 1979), embryonic epidermis (Risek et al., 1994), and between pillar cells in the organ of Corti in the inner ear (Andrew Forge, University College London, personal communication).

Expression of GFP-tagged α_1 (Cx43) monitored over time indicated that expression is initiated in the ER and then accumulated in the Golgi region before the first gap junctions were formed at specific sites of the adjacent membranes, similar to results obtained for wild-type connexins (Musil and Goodenough, 1991; Laird et al., 1991; Laird et al., 1995; Falk et al., 1994). Some intracellular fluorescence detected in α_1 (Cx43)-GFP, β_1 (Cx32)-GFP and β_2 (Cx26)-GFP transfected

Fig. 5. Distribution of channels within gap junctions composed of different connexin isotypes. Connexin isotypes, either CFP (pseudocolored green) or YFP-tagged (pseudocolored red) were cotransfected into HeLa cells as indicated. Stacks of dual-color fluorescence images were acquired, and images were displayed in the projection acquired. Deconvolved images of plaques imaged onto their edge are shown in the left panels. Unprocessed and deconvolved images of plaques imaged onto their plane are shown in the middle and right panels, respectively. Gap junction plaques composed of both connexin isotypes were assembled under these conditions. Connexin isotypes distributed homogeneously throughout the plaque (yellow plaque color) or arranged into well-separated domains (red or green), depending on the connexin isotypes that were coexpressed. Note the structural features of the plaques mentioned in the legend of Fig. 4, and the yellow areas in the unprocessed images of plaques assembled from α_1 (Cx43)/ β_1 (Cx32) and α_1 (Cx43)/ β_2 (Cx26) that disappeared, or were reduced to narrow lines in the border regions between red and green domains in the deconvolved images. Bars, 5 μ m.



HeLa cells, however, did not colocalize with ER and Golgi markers and, therefore, does not represent connexin cargo vesicles in transit to the plasma membrane (visible as green vesicular structures in Fig. 2C, panels 2 and 4). These vesicular structures may include internalized fragments of gap junction plaques destined for degradation (Larsen et al., 1979; Mazet et al., 1985; Severs et al., 1989); alternatively, trafficked connexins (George et al., 1999), mis-targeted fusion proteins or connexin-GFP degradation products. Time-lapse recordings (M. Falk, unpublished data) indicated that the plaques could grow by the addition of channels and by plaque fusion due to lateral movement in the plane of the membrane. Comparable results were also obtained by Jordan et al. (1999) and Holm et al. (1999).

GFP was fused to the C-terminus of connexins since earlier studies showed that deletions (Unger et al., 1999), as well as additions (Sullivan and Lo, 1995) to the C-terminus of connexin subunits were possible without interfering with the intracellular transport, or disrupting assembly of the mutated subunits into gap junction channels and gap junction plaques.

The crystal structure of GFP (Ormö et al., 1996) revealed that its 238 amino acid residues (27 kDa) fold into a tightly packed can 24x42 Å in size. This unique tight structure is believed to be responsible for its inert behavior (Misteli and Spector, 1997). Fig. 7 shows a schematic representation of a gap junction channel drawn to scale that is assembled solely from GFP-tagged connexins. Dimensions were adapted from Makowski et al. (1977) and Unger et al. (1999). The scheme indicates that sufficient space for the six GFP tags is available within the connexon. The electron cryocrystallographic analysis of gap junction channels suggests that the C-terminal domains of the connexin polypeptides form the outer portion of the connexon that faces the cytoplasm (Unger et al., 1999). The N- and C-termini of the GFP polypeptide are located close to each other on one end of the barrel (Ormö et al., 1996). Therefore, it appears likely that the GFP tag simply extends the connexon into the cytoplasm without altering (1) the overall connexon structure, (2) its docking into complete gap junction channels and (3) packing of the channels with their natural spacing of 90Å center to center (Revel and Karnovsky, 1967).

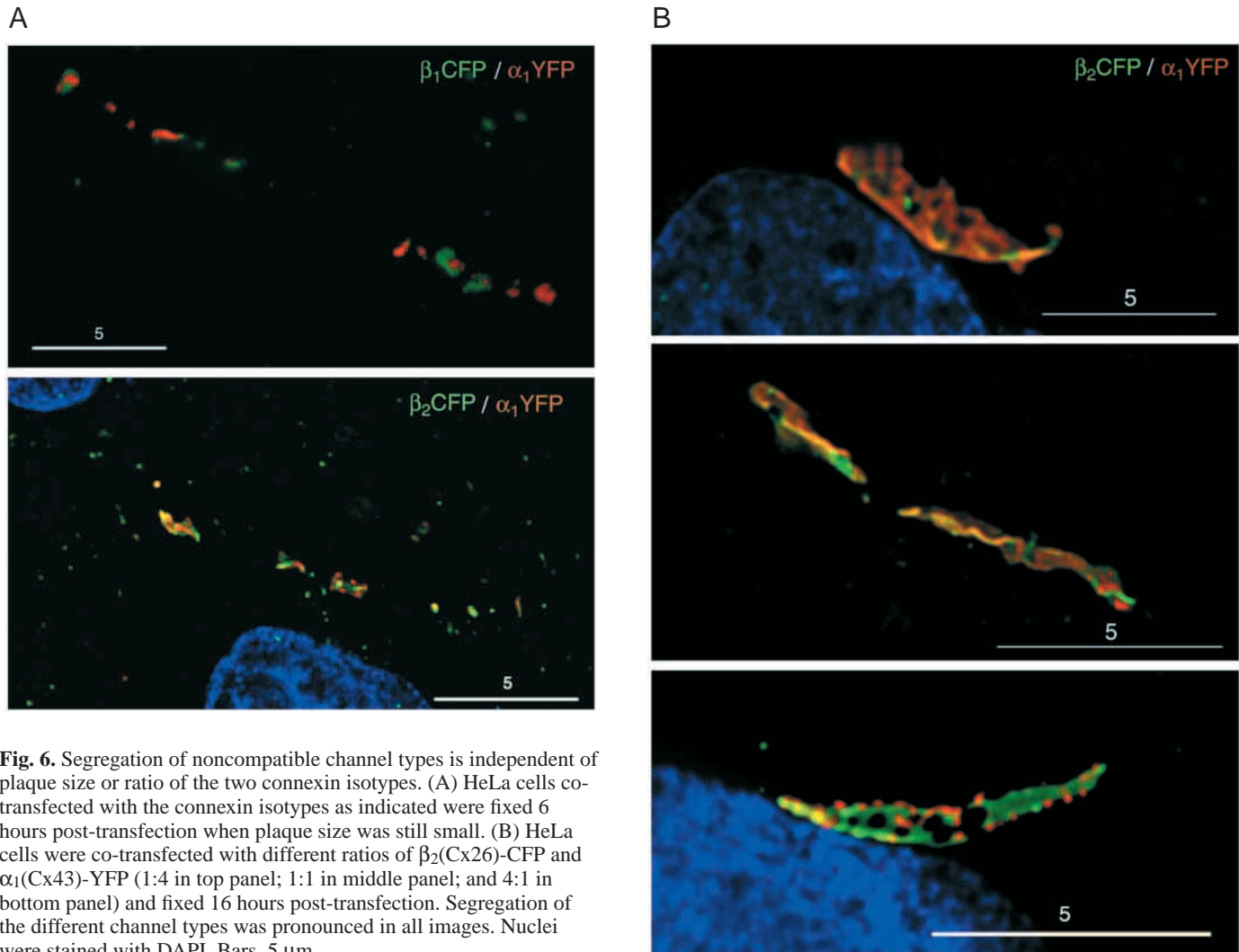


Fig. 6. Segregation of noncompatible channel types is independent of plaque size or ratio of the two connexin isotypes. (A) HeLa cells co-transfected with the connexin isotypes as indicated were fixed 6 hours post-transfection when plaque size was still small. (B) HeLa cells were co-transfected with different ratios of β_2 (Cx26)-CFP and α_1 (Cx43)-YFP (1:4 in top panel; 1:1 in middle panel; and 4:1 in bottom panel) and fixed 16 hours post-transfection. Segregation of the different channel types was pronounced in all images. Nuclei were stained with DAPI. Bars, 5 μm .

This results in two layers of GFP, one on each cytoplasmic side of the adjoining membranes, and in approximately 100,000 tags/ μm^2 . This explains the strong fluorescence of the gap junction plaques, which even allows imaging in the presence of phase-contrast illumination (see Figs 1A, 3). Taken together, our analysis demonstrates that GFP-tagged connexins assemble into functional gap junction channels, and cluster into bona fide gap junctions.

Structure and organization of entire gap junctions in living cells

The detailed structural organization of gap junctions in living cells was investigated by employing high-resolution fluorescence deconvolution microscopy. Predominantly, larger gap junction plaques (2-15 μm in diameter) were investigated since they cannot be confused with vesicular structures and their structural characteristics can better be resolved. However, the same characteristics were also seen in smaller (≤ 2 μm diameter) gap junction plaques (compare Figs 4A,B, 5, rows 2 and 3 left panels and 6A), and in gap junction plaques assembled from stable transfected and endogenous expressed connexins (M. Falk, unpublished results). Gap junction plaques imaged with this technology were found to

be diverse in shape (Fig. 4), typically with wavy or jagged edges and long extending protrusions and deep invaginations. Fluorescent vesicles detected at the edge and in the close vicinity of the plaques, as well as further away in the cytoplasm, probably represent transport vesicles and/or partial plaque degradation products. Striking circular and sometimes irregularly shaped areas (approx. 0.1-1 μm in diameter) deprived of gap junction channels that could move quite rapidly were found within the plaques. Such channel-free areas were first described by freeze-fracture electron microscopy and were termed nonjunctional membranes (Friend and Gilula, 1972). Currently, we are investigating the nature, significance and dynamics of these nonjunctional membrane areas.

Volume rendering of entire z-section stacks enabled us to transform gap junction plaques, so far only imaged as one-dimensional puncta, lines or fragmental sheets with conventional imaging techniques, into complete three-dimensional structures, thereby demonstrating for the first time how gap junctions appear in the adjoining membranes between living cells. The volume reconstructions were further animated to better demonstrate the gap junction plaque structure (see attached QuickTime movie sequences 1-5).

Marzillier, Danuta Balicki and Ben Giepmans for their scientific discussion and critical suggestions. This work was supported by grant RO1 GM55725 from the National Institute of Health to M.M.F. M.M.F. is a former recipient of a Deutsche Forschungsgemeinschaft fellowship Fa 261/1-1.

REFERENCES

- Agard, D. A., Hiraoka, Y., Shaw, P. and Sedat, J. W. (1989). Fluorescence microscopy in 3 dimensions. *Meth. Cell Biol.* **30**, 353-377.
- Axelrod, D., Ravdin, P., Koppel, D. E., Schlessinger, J., Webb, W. W., Elson, E. L. and Podleski, T. R. (1976). Lateral motion of fluorescently labeled acetylcholine receptors in membranes of developing muscle fibers. *Proc. Natl. Acad. Sci. USA* **73**, 4594-4598.
- Bevans, C. G., Kordel, M., Rhee, S. K. and Harris, A. L. (1998). Isoform composition of connexin channels determines selectivity among second messengers and uncharged molecules. *J. Biol. Chem.* **273**, 2808-2816.
- Brink, P. R., Cronin, K., Banach, K., Peterson, E., Westphale, E. M., Seul, K. H., Ramanan, S. V. and Beyer, E. C. (1997). Evidence for heteromeric gap junction channels formed from rat connexin43 and human connexin37. *Am. J. Physiol.* **273**, C1386-1396.
- Bruzzone, R., White, T. W. and Goodenough, D. A. (1996a). The cellular Internet: on-line with connexins. *BioEssays* **18**, 709-718.
- Bruzzone, R., White, T. W. and Paul, D. L. (1996b). Connections with connexins: the molecular basis of direct intercellular signaling. *Eur. J. Biochem.* **238**, 1-27.
- Bukauskas, F. F., Jordan, K., Bukauskiene, A., Bennett, M. V., Lampe, P. D., Laird, D. W. and Verselis, V. K. (2000). Clustering of connexin 43-enhanced green fluorescent protein gap junction channels and functional coupling in living cells. *Proc. Natl. Acad. Sci. USA* **97**, 2556-2561.
- Dunia, I., Manenti, S., Rousselet, A. and Benedetti, E. L. (1987). Electron microscopic observations of reconstituted proteoliposomes with the purified major intrinsic membrane protein of eye lens fibers. *J. Cell Biol.* **105**, 1679-1689.
- Eckert, R., Dunina-Barkovskaya, A. and Hülser, D. F. (1993). Biophysical characterization of gap junction channels in HeLa cells. *Pflügers Archiv.* **205**, 404-407.
- Elfgang, C., Eckert, R., Lichtenberg-Fraté, H., Butterweck, A., Traub, O., Klein, R., Hülser, D. and Willecke, K. (1995). Specific permeability and selective formation of gap junction channels in connexin-transfected HeLa cells. *J. Cell Biol.* **129**, 805-817.
- Falk, M. M. (2000a). Cell-free synthesis for analyzing the membrane integration, oligomerization and assembly characteristics of gap junction connexins. *Methods* **20**, 165-179.
- Falk, M. M. (2000b). Biosynthesis and structural composition of gap junction intercellular membrane channels. *Eur. J. Cell Biol.* **79**, 564-574.
- Falk, M. M., Buehler, L. K., Kumar, N. M. and Gilula, N. B. (1997). Cell-free synthesis of connexins into functional gap junction membrane channels. *EMBO J.* **10**, 2703-2716.
- Falk, M. M., Buehler, L. K., Kumar, N. M. and Gilula, N. B. (1998). Cell-free expression of functional gap junction channels. In *Gap Junctions* (ed. R. Werner), pp. 135-139. Amsterdam: IOS Press.
- Falk, M. M. and Gilula, N. B. (1998). Connexin membrane protein biosynthesis is influenced by polypeptide positioning within the translocon and signal peptidase access. *J. Biol. Chem.* **273**, 7856-7864.
- Falk, M. M., Kumar, N. M., and Gilula, N. B. (1994). Membrane insertion of gap junction connexins: polytopic channel forming membrane proteins. *J. Cell Biol.* **127**, 343-355.
- Falk, M. M. and Lauf, U. (2000). High resolution, fluorescence deconvolution microscopy and tagging with the autofluorescent tracers CFP, GFP, and YFP to study the structure and function of gap junctions in living cells. *Microsc. Res. Tech.* (in press).
- Friend, D. S. and Gilula, N. B. (1972). Variations in tight and gap junctions in mammalian tissues. *J. Cell Biol.* **53**, 758-776.
- George, C. H., Kendall, J. M. and Evans, W. H. (1999). Intracellular trafficking pathways in the assembly of connexins into gap junctions. *J. Biol. Chem.* **274**, 8678-8685.
- Gil, T., Ipsen, J. H., Mouritsen, O. G., Sabra, M. C., Sperotto, M. M. and Zuckermann, M. J. (1998). Theoretical analysis of protein organization in lipid membranes. *Biochim. Biophys. Acta* **1376**, 245-266.
- Gilula, N. B., Reeves, O. R. and Steinbach, A. (1972). Metabolic coupling, ionic coupling and cell contacts. *Nature* **235**, 262-265.
- Ginzberg, R. D. and Gilula, N. B. (1979). Modulation of cell junctions during differentiation of the chicken otocyst sensory epithelium. *Dev. Biol.* **68**, 110-129.
- Goodenough, D. A., Goliger, J. A. and Paul, D. L. (1996). Connexins, connexons, and intercellular communication. *Annu. Rev. Biochem.* **65**, 475-502.
- He, D. S., Jiang, J. X., Taffet, S. M. and Burt, J. M. (1999). Formation of heteromeric gap junction channels by connexins 40 and 43 in vascular smooth muscle cells. *Proc. Natl. Acad. Sci. USA* **96**, 6495-6500.
- Holm, I., Mikhailov, A., Jillson, T. and Rose, B. (1999). Dynamics of gap junctions observed in living cells with connexin43-GFP chimeric protein. *Eur. J. Cell Biol.* **78**, 856-866.
- Hülser, D. F., Rehkopf, B. and Traub, O. (1997). Dispersed and aggregated gap junction channels identified by immunogold labeling of freeze-fractured membranes. *Exp. Cell Res.* **233**, 240-251.
- Jiang, J. X. and Goodenough, D. A. (1996). Heteromeric connexons in lens gap junction channels. *Proc. Natl. Acad. Sci. USA* **93**, 1287-1291.
- Jordan, K., Solan, J. L., Dominguez, M., Sia, M., Hand, A., Lampe, P. D. and Laird, D. W. (1999). Trafficking, assembly, and function of a connexin43-green fluorescent protein chimera in live mammalian cells. *Mol. Biol. Cell* **10**, 2033-2050.
- Kumar, N. M. and Gilula, N. B. (1996). The gap junction communication channel. *Cell* **84**, 381-388.
- Laird, D. W., Puranam, K. and Revel, J.-P. (1991). Turnover and phosphorylation dynamics of connexin 43 gap junction protein in cultured cardiac myocytes. *Biochem. J.* **272**, 67-72.
- Laird, D. W., Castillo, M. and Kasprzak, L. (1995). Gap junction turnover, intracellular trafficking, and phosphorylation of connexin43 in brefeldin A-treated rat mammary tumor cells. *J. Cell Biol.* **131**, 1193-1203.
- Larsen, W. J., Tung, Murray, H.-N., S. A. and Swenson, C. A. (1979). Evidence for the participation of actin microfilaments and bristle coats in the internalization of gap junction membrane. *J. Cell Biol.* **83**, 576-587.
- Makowski, L., Caspar, D. L. D., Phillips, W. C. and Goodenough, D. A. (1977). Gap junction structures. *J. Cell Biol.* **74**, 629-645.
- Mazet, F., Wittenberg, B. A. and Spray, D. C. (1985). Fate of intercellular junctions in isolated adult rat cardiac cells. *Circ. Res.* **56**, 195-204.
- McNutt, N. S. and Weinstein, R. S. (1970). The ultrastructure of the nexus. A correlated thin-section and freeze-cleavage study. *J. Cell Biol.* **47**, 666-688.
- Milks, L. C., Kumar, N. M., Houghten, N., Unwin, N. and Gilula, N. B. (1988). Topology of the 32-kD liver gap junction protein determined by site-directed antibody localizations. *EMBO J.* **7**, 2967-2975.
- Misteli, T. and Spector, D. L. (1997). Applications of the green fluorescent protein in cell biology and biotechnology. *Nat. Biotech.* **15**, 961-964.
- Musil, L. S. and Goodenough, D. A. (1991). Biochemical analysis of connexin43 intracellular transport, phosphorylation, and assembly into gap junction plaques. *J. Cell Biol.* **115**, 1357-1374.
- Ormö, M., Cubitt, A. B., Kallio, K., Gross, L. A., Tsien, R. Y. and Remington, S. J. (1996). Crystal structure of the *Aequorea victoria* green fluorescent protein. *Science* **273**, 1392-1395.
- Peng, H. B. (1983). Cytoskeletal organization of the presynaptic nerve terminal and the acetylcholine receptor cluster in cell cultures. *J. Cell Biol.* **97**, 489-498.
- Rash, J. E., Staehelin, L. A. and Ellisman, M. H. (1974). Rectangular arrays of particles on freeze-cleaved plasma membrane are not gap junctions. *Exp. Cell Res.* **86**, 187-190.
- Revel, J.-P. and Karnovsky, M. J. (1967). Hexagonal array of subunits in intracellular junctions of the mouse heart and liver. *J. Cell Biol.* **33**, C7-C12.
- Risek, B., Klier, G. F. and Gilula, N. B. (1994). Developmental regulation and structural organization of connexins in epidermal gap junctions. *Dev. Biol.* **164**, 183-196.
- Severs, N. J., Shovel, K. S., Slade, A. M., Powell, T., Twist, V. W. and Green, C. R. (1989). Fate of gap junctions in isolated adult mammalian cardiomyocytes. *Circ. Res.* **65**, 22-42.
- Shaw, P. J. (1998). Computational deblurring of fluorescence microscope images. In *Cell Biology: A Laboratory Handbook*, Second Edition: Vol. 3 (ed. J. E. Celis), pp. 206-217. Academic Press, San Diego.
- Sosinsky, G. (1995). Mixing of connexins in gap junction membrane channels. *Proc. Natl. Acad. Sci. USA* **92**, 9210-9214.
- Sosinsky, G. E. (1996). Molecular organization of gap junction membrane channels. *J. Bioenerg. Biomembr.* **28**, 297-309.
- Stauffer, K. A. (1995). The gap junction proteins β 1-connexin (connexin-32) and β 2-connexin (connexin-26) can form heteromeric hemichannels. *J. Biol. Chem.* **270**, 6768-6772.
- Sullivan, R. and Lo, C. W. (1995). Expression of a connexin 43/beta-galactosidase fusion protein inhibits gap junctional communication in NIH3T3 cells. *J. Cell Biol.* **130**, 419-429.
- Tsukita, S. and Furuse, M. (1999). Occludin and claudins in tight-junction strands: leading or supporting players? *Trends Cell Biol.* **9**, 268-273.
- Tsukita S. and Furuse, M. (2000). Pores in the wall. Claudins constitute tight junction strands containing aqueous pores. *J. Cell Biol.* **149**, 13-16.
- Unger, V. M., Kumar, N. M., Gilula, N. B. and Yeager, M. (1999). Three-dimensional structure of a recombinant gap junction membrane channel. *Science* **283**, 1176-1180.
- Yang, B., Brown, D. and Verkman, A. S. (1996). The mercurial insensitive water channel (AQP-4) forms orthogonal arrays in stably transfected chinese hamster ovary cells. *J. Biol. Chem.* **271**, 4577-4580.
- Yeager, M., Unger, V. M. and Falk, M. M. (1998). Synthesis, assembly and structure of gap junction intercellular channels. *Curr. Opin. Struct. Biol.* **8**, 517-524.